

Photovoltaic System Power Reserve Determination Using Parabolic Approximation of Frequency Response

Tomislav Baškarad^{ib}, Graduate Student Member, IEEE, Igor Kuzle^{ib}, Senior Member, IEEE, Ninoslav Holjevac^{ib}, Member, IEEE

Abstract—The most commonly used method for including photovoltaic system in the control of system frequency is to operate a PV power plant at reduced power while maintaining a specific amount of available power reserve. Such operating regime, often referred to as de-loaded, can cause additional costs and, consequently, determining a required power reduction becomes vitally important. This paper introduces a method for determining the required minimum de-loaded reserve of a photovoltaic system. To achieve the desired result a parabolic approximation of the system frequency response is developed to derive an explicit function of the frequency nadir. Taking this approximation into consideration, a method for determining the required minimum de-loaded margin was developed and tested in a case-study which observed a small power system consisting of several power plants. To demonstrate the accuracy of the proposed parabolic approximation, the calculated approximate values of the frequency nadir were compared to the values of the frequency nadir obtained from the frequency response simulations performed on the power system model developed in MATLAB/Simulink.

Index Terms—Parabolic approximation, frequency response, power reserve, de-loaded margin, photovoltaic system.

NOMENCLATURE

a, b, c	Coefficients of the parabola.
$a_{base}, b_{base}, c_{base}$	Coefficients of the parabola for the base case.
$C(s)$	Converter system transfer function.
C, L	Converter capacitance and inductance.
d	Moment at which photovoltaic system reaches a maximum output.
D	Load damping constant.
ε	Damping factor.

f	Power system frequency.
Δf	Power system frequency deviation.
$F_{ass}(s)$	Laplace transform of the function $f_{ass}(t)$.
$f_{ass}(t)$	Assumed quadratic function of system frequency.
$f_{ass}'(t)$	Derivation of the assumed quadratic function of frequency.
F_{HP}	Fraction of the power.
f_{min}	System frequency minimum, i.e., minimum of a parabola.
$f_{min-base}$	System frequency minimum of the base power system.
f_n	Nominal system frequency.
f_{nadir}	System frequency nadir.
$f_{sys}(t)$	System frequency solution.
H	System inertia constant.
H_n	Decreased system inertia constant.
$HPP(s), TPP(s), PV(s)$	Transfer functions of the hydro, thermal and photovoltaic power plant
I_{pv}, V_{pv}	Current and voltage of the PV plant.
k	System inertia reduction coefficient.
K_0	PV transfer function gain.
K_p, K_i	PI controller coefficients.
$\mathcal{L}, \mathcal{L}^{-1}$	Laplace transform/inverse Laplace transform.
P_{HPP}, P_{TPP}, P_{PV}	Nominal power of the hydro, thermal and photovoltaic power plant.
P_B	System base power.
P_L	Step load disturbance.
$P_{PVPP}(t)$	Photovoltaic power response in the time domain.
P_r	Photovoltaic system power reserve.
$PV_{new}(s)$	Transfer function of the photovoltaic power plant which considers the limitation of the power reserve.
R_H, R_T, R_{pv}	Droop constant of the hydro, thermal and photovoltaic power plant.
r_{pv}	Dynamic resistance of the photovoltaic power plant.
R_T	Transient droop.
s	Laplace variable.
t	Time.

Manuscript received January 30, 2020; revised August 3, 2020 and November 19, 2020; accepted February 20, 2021. Date of publication February 24, 2021; date of current version June 21, 2021. This work was supported in part by the Croatian Science Foundation under the Project WINDLIPS—WIND energy integration in Low Inertia Power System under Grant HRZZ-PAR-02-2017-03, and in part by the H2020 Project CROSSBOW—CROSS Border Management of Variable Renewable Energies and Storage Units Enabling a Transnational Wholesale Market under Grant 773430. Paper no. TSG-00144-2020. (Corresponding author: Tomislav Baškarad.)

The authors are with the Faculty of Electrical Engineering and Computing, University of Zagreb, 10000 Zagreb, Croatia (e-mail: tomislav.baskarad@fer.hr; igor.kuzle@fer.hr; ninoslav.holjevac@fer.hr).

Color versions of one or more figures in this article are available at <https://doi.org/10.1109/TSG.2021.3061893>.

Digital Object Identifier 10.1109/TSG.2021.3061893

t_1, t_2, t_3	Three different points for the parabola determination.
T_{CH}	Control valve time constant.
T_d	Time delay constant.
T_G	Governor time constant.
t_{nadir}	Time of frequency nadir.
T_R	Reset time.
T_{RH}	Reheater time constant.
T_W	Turbine time constant.
$u(t)$	Heaviside step function.
V_{dc}	DC link voltage.
ω_0	Undamped natural frequency.

I. INTRODUCTION

ACCORDING to the International Energy Agency report [1], at the end of 2019, the total capacity of installed photovoltaic (PV) systems in the world was around 620 GW. In 2020, an additional 140 GW of PV systems is expected to be installed. The continuation of such rapid growth in installed PV capacity and the increase in the share of PV systems could negatively impact the power system operation and potentially threaten the system stability. The reasons for concern are: a lack of rotational mass in PV plants, which causes minimal contribution to the overall system inertia [2], and, the operation in the Maximum Power Point Tracking (MPPT) mode means there is no power reserve available for frequency control.

The literature dealing with the possibilities of PV participation in system frequency regulation can be classified into two main groups. The first group consists of papers suggesting combining PV systems with a particular energy storage device, for example, a DC-link capacitor [3] or a battery [4], both able to provide fast power reserve. The second group of papers propose the operation of PV plants at the output power below maximum power point, in the so-called de-loaded mode, thereby providing a certain amount of power reserve. The drawback of the first potential solution is the increase in installation costs and because of the high energy storage price. The drawback of the second suggested group of solutions is the increase in operating costs and the potential loss of production due to operation at a sub-optimal point. While there are many existing papers [5]–[8] focusing on the optimal sizing of energy storage in order to minimize costs; the literature on analyzing and calculating the appropriate PV power reserve, i.e., de-loaded margin of PV systems, is still relatively rare.

Some papers, such as [9]–[11], propose only the power reserve control strategy for PV systems without discussing the amount of actual power reserve that needs to be controlled. It has been shown that the reference power reserve can be maintained either at the fixed amount [9] or at the amount equal to a fixed percentage of the maximum available power [10]. Generally speaking, the amount of desired power reserve can be set to any given reference point within the interval from near-zero to 100% of the available power [11]. Furthermore, a PV power reserve can be controlled without additional hardware, as shown in [12]. In papers investigating the improvements in frequency stability due to PV systems

participation in the frequency control a fixed de-loaded margin is usually used. In [13]–[15] the de-loaded margin is predefined as 10% while in [16], 20% of the nominal power was selected arbitrarily and without any further explanation. The predefined PV de-loaded margin value of 10% is also used for projects carried out in large-scale PV plants in order to test their ability to provide ancillary service to the grid as described in [17].

In [18], a wide-area measurement system (WAMS)-based method is proposed to calculate a PV power reserve margin. According to this reference, the PV system de-loaded margin was calculated to be over 40% which led to unacceptably high costs. Furthermore, the study conducted in [19] showed that maintaining a PV power reserve level in the interval of 10-20% is sufficient to improve the system frequency response with a reasonable costs increase. On the other hand, in [20], an amount of active power reserve created from curtailment is not set to a fixed percentage but dynamically adjusted in the intervals from 2.8% to 22.5% depending on the PV plant size. Unfortunately, the impact on the system frequency control was not examined. Similar approach was taken in [21] where the de-loaded margin of the PV system is dynamically changed considering a 10 minute solar irradiation forecasts and the operating conditions of the system. However, the explanation of the selection process for obtaining the reserve values is missing. Also, both of these papers provide little or no discussion regarding the impact the de-loaded margin has on the amount of power reserve availability.

This paper presents a viable method for determining the de-loaded margin of the PV system required to maintain the frequency stability. The amount of power reserve required to preserve the frequency stability is closely correlated with the frequency nadir. The fundamental idea is to establish a mathematical relationship between the frequency nadir and the system parameters; such as, system inertia, load disturbance, PV power reserve, etc. In the existing literature several methods for developing the analytical expression of the nadir function can be found [22]–[26].

In [22], the authors derive the analytical expression of the frequency nadir function for the single-machine power system model with a reheat turbine. Similarly, the frequency nadir function for the multi-machine (with reheat turbines) power system model is derived in [23]. However, in order to derive the explicit frequency-nadir function, the model of a multi-machine power system must consist of the identical type of generating units. Therefore, the method presented in [23] cannot be applied to a mixed power generation system. For this method to be feasible a low-order heat turbine model is necessary.

The model presented in [24] takes into account the response of various types of generating units but only a first-order transfer function is used to approximate the real power plant response. The simple method for determining frequency nadir as a function of the system parameters is proposed in [25] assuming the delivery of primary frequency response can be modelled as a linear function. This paper, however, does not consider the various turbine models. The research presented in [26] expands the multi-machine power system model used

in [23] by incorporating the impact of grid-forming converters. The realization of this method still requires the use of the low-order turbine models.

Generally, the methods for the analytical derivation of frequency nadir function presented in the literature can be classified into two main groups according to the type of power system and the turbine models used:

1) single-machine power system model with full-order turbine model;

2) multi-machine power system model with low-order turbine model.

To the best of our knowledge, the derivation of an analytical function of the frequency nadir for the multi-machine power system with the full-order turbine models has not been presented before. Therefore, obtaining an explicit function of the frequency nadir with the method we propose can make a valuable contribution. The novelty of the method is that it can be applied to the multi-machine power system model consisting of various types of generating units, and its utilization of the full-order turbine models. Additionally, the method is not computationally demanding and shows a high degree of accuracy compared to the values obtained from the conducted power system simulations. The analyzed power system model includes hydro, thermal, and photovoltaic generation technologies. Furthermore, there are no limitations excluding other technologies such as the wind power plant model presented in [27].

In summary, the main contributions of this paper are:

- Development of a parabolic approximation of the system frequency response;
- Establishment of the frequency nadir as an explicit function of system inertia and PV power reserve;
- Determination of the required minimum PV power reserve to maintain the system frequency stability.

This paper is structured as follows: In Section II, a method for parabolic frequency response approximation is developed. Section III describes the determination of the required minimum PV power reserve margin. Section IV presents the results, and Section V concludes the paper.

II. FREQUENCY RESPONSE PARABOLIC APPROXIMATION

A. Generation Unit Models

The model of hydropower generating unit is represented with the governor, the transient droop compensation, and the turbine transfer functions [28]:

$$HPP(s) = \frac{1}{R_H} \cdot \frac{1}{1+sT_G} \cdot \frac{1+sT_R}{1+s\left(\frac{R_T}{R_H}\right)T_R} \cdot \frac{1-sT_W}{1+0.5sT_W} \quad (1)$$

The model of thermal generating unit with a reheat turbine cycle is represented with the governor and the turbine transfer functions [28]:

$$TPP(s) = \frac{1}{R_T} \cdot \frac{1}{1+sT_G} \cdot \frac{1+sF_{HP}T_{RH}}{(1+sT_{CH})(1+sT_{RH})} \quad (2)$$

Unlike the conventional power plant models which are well known and widely used, a generic PV system model convenient for system frequency response analysis has not yet been adopted. In general, the PV system active power change can be represented as (3):

$$\Delta P_{pv}(s) = \Delta\omega(s) \cdot \frac{1}{R_{pv}} \cdot C(s) \quad (3)$$

where $\Delta\omega(s)$ is the frequency deviation, R_{pv} is the droop constant, and $C(s)$ is the converter system transfer function. In the literature [22], [29], $C(s)$ is usually set to the value of 1 as the converter dynamics are much faster than the governor-turbine actions. However, in this paper, a more accurate $C(s)$ representation [11] will be used. It is represented by a PI controller, delay, and typical second-order transfer function.

$$C(s) = \frac{\frac{1}{P_{pv}} \cdot \left(K_p + \frac{K_i}{s}\right) \cdot \frac{2-T_{ds}}{2+T_{ds}} \cdot \frac{K_0}{s^2+2e\omega_0s+\omega_0^2}}{1 + \frac{1}{P_{pv}} \cdot \left(K_p + \frac{K_i}{s}\right) \cdot \frac{2-T_{ds}}{2+T_{ds}} \cdot \frac{K_0^2}{s} + 2e\omega_0s + \omega_0^2} \quad (4)$$

K_0 , e and, ω_0 are given by:

$$K_0 = \frac{-V_{dc}}{LC} \left(I_{pv} + \frac{V_{pv}}{r_{pv}} \right) \quad (5)$$

$$\omega_0 = \frac{1}{\sqrt{LC}} \quad (6)$$

$$\varepsilon = \frac{-1}{2 \cdot r_{pv} \cdot C\omega_0} \quad (7)$$

Finally, by inserting the real parameter values, which are listed in Table III of the Appendix, into equation (4) the transfer function of the PV system participating in frequency control is obtained:

$$PV(s) = \frac{1}{R_{pv}} \times \frac{1.385 \cdot 10^6 s^2 + 5.47 \cdot 10^{10} s + 2.77 \cdot 10^{13}}{s^4 + 40710s^3 + 3.127 \cdot 10^7 s^2 + 2.249 \cdot 10^{11} s + 2.77 \cdot 10^{13}} \quad (8)$$

B. Methodology

Ordinarily, the single-area multi-machine power system model convenient for exploring and simulating the frequency response is derived in Laplace s -domain. Transforming the model from Laplace s -domain to the time domain leads to the following equation:

$$\Delta f(t) = \mathcal{L}^{-1} \left\{ \frac{P_L(s)}{2Hs + D + \sum_{i=1}^n \frac{1}{R_{Hi}} HPP(s)_i + \sum_{i=1}^m \frac{1}{R_{Ti}} TPP(s)_i + \sum_{i=1}^k \frac{1}{R_{pvi}} PV(s)_i} \right\} \quad (9)$$

where Δf is the system frequency deviation; t is time; \mathcal{L}^{-1} denotes the inverse Laplace transform; $HPP(s)_i$, $TPP(s)_i$, and $PV(s)_i$ are the transfer functions of the i^{th} hydropower generating unit, thermal power generating unit, and photovoltaic power plant respectively; n , m , and k represent the number of hydropower plants, thermal power plants, and photovoltaic power plants in the system respectively; R_{Hi} , R_{Ti} , and R_{pvi} are droop constants of the i^{th} hydro, thermal, and photovoltaic power plant; P_L is a step load disturbance; H is the system

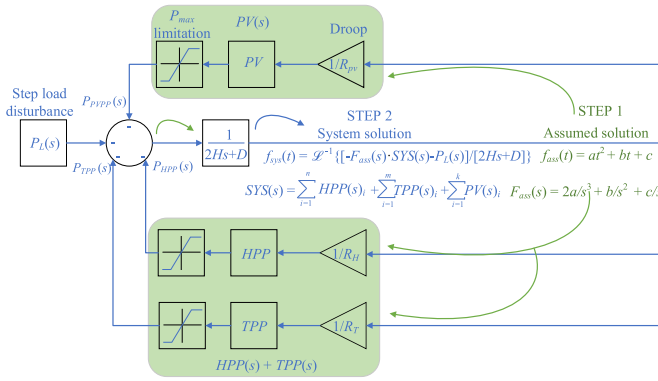


Fig. 1. Concept of developing frequency response parabolic approximation.

inertia constant; D is the load damping constant. Solving (9) is very demanding and it can be numerically calculated only if all the parameters are known. Furthermore, it is impossible to express the frequency nadir as an explicit function of the system parameters (e.g., H , P_L , R , etc.) by solving (9).

To obtain a mathematical relationship between the frequency nadir and the system parameters in the time domain, a parabolic approximation of the system frequency response following a load disturbance had to be developed. Only after parabolic approximation was developed, the analysis of the dependence of the frequency nadir on the system parameters could be performed.

The idea behind the parabolic approximation of system nadir stems from the observation that the general frequency response curve in the part of the frequency response from $t = 0$ (a start of frequency drop) to $t = t_{nadir}$ resembles one half of the parabolic curve. This novel concept of devising frequency response parabolic approximation is depicted in Fig. 1. Assuming the solution, frequency versus time, of the system differential equation is in the form of the quadratic equation, obtained by transforming the power system model (Fig. 1) from Laplace s -domain to the time domain, it can be written as:

$$f_{ass}(t) = at^2 + bt + c \quad (10)$$

where f_{ass} is the assumed function of frequency, t is the time, and the numbers a , b , and c are the coefficients of the quadratic equation.

Starting from the assumed solution of the system frequency f_{ass} , the system solution can be written as:

$$f_{sys}(t) = \mathcal{L}^{-1} \left\{ [-F_{ass}(s) \cdot [SYS(s)] - P_L(s)] \frac{1}{2Hs + D} \right\} \quad (11)$$

$$SYS(s) = \sum_{i=1}^n HPP(s)_i + \sum_{i=1}^m TPP(s)_i + \sum_{i=1}^k PV(s)_i \quad (12)$$

where $F_{ass}(s)$ is a Laplace transform of the assumed solution $f_{ass}(t)$. As can be seen from (12), the power system model shown in Fig. 1 can consist of several power plants and each would be modelled with its own transfer function and taken into consideration in the total system equation (11). However, for clarity and simplicity, just one block of HPP s, TPP s, and PV s is shown in Fig. 1.

After the quadratic solution (10) is assumed, the quadratic coefficients a , b , and c need to be determined. Since the assumed solution f_{ass} and the system solution f_{sys} represent the same frequency response, the quadratic coefficients can be found by setting the responses:

$$f_{ass}(t) = f_{sys}(t) \quad (13)$$

The quadratic equation is determined by three points. Inputting the three different values t_1 , t_2 , t_3 for t into (13), the system of three equations with three variables (a , b , c) is obtained with a unique solution.

C. Selecting the t_1 , t_2 , t_3

Although the values t_1 , t_2 , and t_3 cannot be arbitrarily chosen, there are numerous sets of (t_1 , t_2 , t_3) which can achieve satisfactory results. One method for providing the selection of appropriate values t_1 , t_2 , and t_3 is described here. Considering that the parabola mainly approximates the inertial response part of the frequency curve, whose time frame is usually up to a few seconds [30], it is reasonable to select values for t_1 , t_2 and t_3 from these intervals. Additionally, the values are permutable so if the selected values $t_1 = 1$, $t_2 = 2$, $t_3 = 3$ are a valid triplet, then the following permuted values are also valid: $t_1 = 2$, $t_2 = 3$, $t_3 = 1$ or similarly $t_1 = 3$, $t_2 = 1$, $t_3 = 2$ etc.

In particular, this paper shows t_1 , t_2 , and t_3 were determined specifically for the power system which was used to analyze the required minimum PV power reserve. The considered 1 GW power system consists of one thermal power plant ($P_{TPP} = 300$ MW) and three hydropower plants ($P_{HPP1} = 250$ MW, $P_{HPP2} = 250$ MW, $P_{HPP3} = 200$ MW). Other parameters are given in Table II of the Appendix. It should be noted that droop has to be expressed in per unit of the system as:

$$R[p.u.] = \frac{R[\%] P}{100 P_B} \quad (14)$$

where P is the nominal power of the power plant [MW], P_B is the system base power [MW], and R [%] is droop of the generator.

Additionally, D is set to 0 for simplicity. The method is performed in several steps.

1st step: Arbitrarily choose any value within the interval from 0 to 4 seconds and insert it as t into (13). In this case, the value 0.1 was chosen.

$$t_1 = 0.1 \rightarrow \text{Eq. (13)} (H=3, P_L=0.05) \Rightarrow f_1(a, b, c) = \text{const.}$$

2nd step: Set several different values for $t_j = t_1$ into (13) and for each of them obtain the second equation $f_2(a, b, c) = \text{const.}$ In this case, the following values were chosen:

$$t_{21} = 1.5 \quad f_{21}(a, b, c) = \text{const.}$$

$$t_{22} = 2 \rightarrow \text{Eq. (13)} (H=3, P_L=0.05) \Rightarrow f_{22}(a, b, c) = \text{const.}$$

$$t_{23} = 2.5 \quad f_{23}(a, b, c) = \text{const.}$$

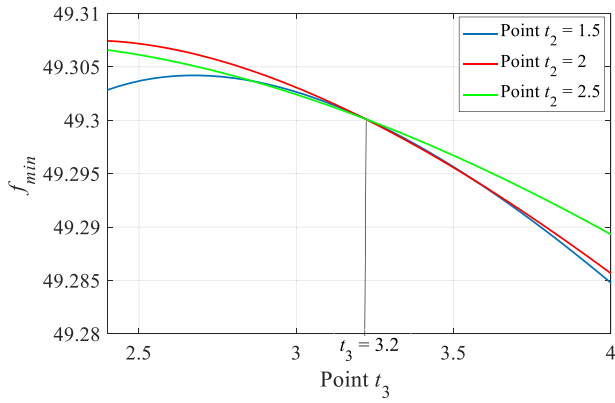


Fig. 2. Curves depicting the process of obtaining the point t_3 .

3rd step: Set $t = t_3$ for t into (13) to obtain the third equation $f_3(a, b, c, t_3) = \text{const}$.

$t = t_3 \rightarrow \text{Eq. (13)} (H=3, P_L = 0.05) \Rightarrow f_3(a, b, c, t_3) = \text{const}$.

4th step: Solve the systems of three equations f_1, f_2k , and $f_3, k = 1, 2, 3$ for a, b, c and obtain the minimum value as a function of t_3 :

$$\begin{aligned} f_{\min}(t_3) &= \left(c - \frac{b^2}{4a} + 1 \right) \cdot f_n \\ (f_1, f_{21}, f_3) &\rightarrow a, b, c \rightarrow f_{\min1}(t_3) \\ (f_1, f_{22}, f_3) &\rightarrow a, b, c \rightarrow f_{\min2}(t_3) \\ (f_1, f_{23}, f_3) &\rightarrow a, b, c \rightarrow f_{\min3}(t_3) \end{aligned} \quad (15)$$

5th step: Find t_3 as the intersection point of the functions $f_{\min1}, f_{\min2}, f_{\min3}$ (see Fig. 2). In the observed case, for the above selected values, the point $t_3 = 3.2$ is obtained.

When the two points are known, $t_1 = 0.1$ and $t_3 = 3.2$, it is necessary to find point t_2 . It can be done in the following steps:

1st step: Obtain the functions f_1, f_2, f_3 as:

$$\begin{aligned} t_1 = 0.1 & \quad f_1(a, b, c, H) = \text{const.} \\ t = t_2 \rightarrow \text{Eq. (13)} (H = H, P_L = 0.05) & \Rightarrow f_2(a, b, c, H, t_2) = \text{const.} \\ t_3 = 3.2 & \quad f_3(a, b, c, H) = \text{const.} \end{aligned}$$

2nd step: Solve the system of three equations f_1, f_2 , and f_3 for a, b, c and obtain the minimum value $f_{\min}(H, t_2)$ as a function of H and t_2 using (15)

3rd step: Draw the graphs of the functions $f_{\min}(H, t_2)$ for several H (e.g., $H = 3, H = 4, H = 5, H = 6$) (see Fig. 3). It is evident from Fig. 3 that for any point t_2 , from the interval 1.5 to 3, the minimum value is not significantly changed. Accordingly, the midpoint of the interval was chosen, i.e., $t_2 = 2.2$. If value of the frequency minimum deviates significantly for various points t_2 , there are no valid sets (t_1, t_2, t_3) where $t_1 = 0.1$. Therefore, a different value for t_1 should be chosen, e.g., $t_1 = 0.2$, and a new set should be obtained.

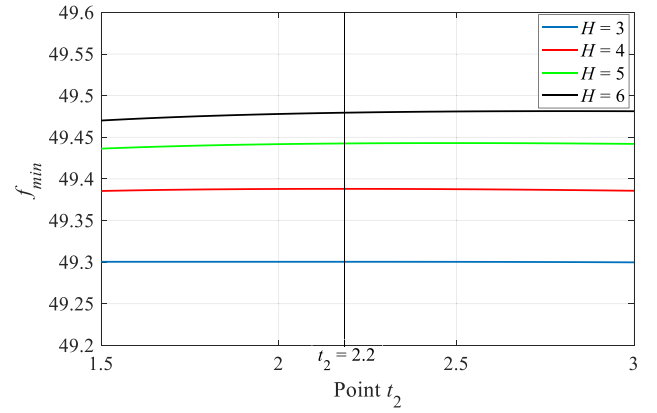


Fig. 3. Process of obtaining the point t_2 .

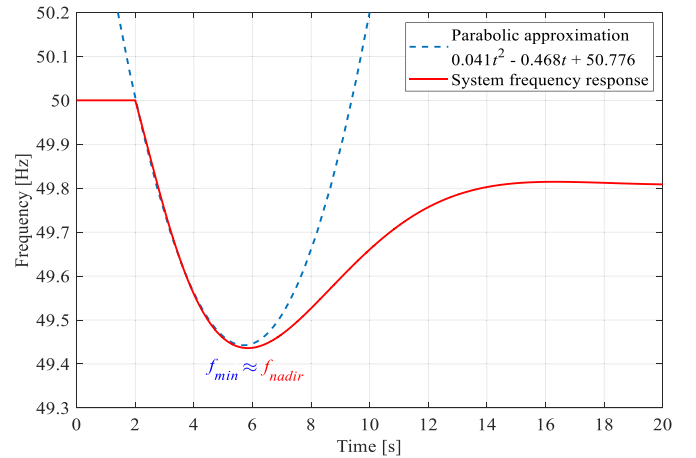


Fig. 4. System frequency response approximated with a parabolic function.

D. Method Accuracy Evaluation

To show the accuracy of the proposed method, a parabolic approximation of the frequency response was calculated considering the above-mentioned 1 GW power system. Inserting $t_1 = 0.1, t_2 = 2.2$, and $t_3 = 3.2$ into (13), along with parameters $H = 5$ and $P_L = 0.05$, the following coefficients of the quadratic equation were obtained: $a = 0.000820, b = -0.006077, c = 0.000098$. Recalling (10), the quadratic function of the frequency deviation in per unit can be written as:

$$\Delta f(t) = 0.00082t^2 - 0.006077t + 0.000098 \quad (16)$$

The quadratic function of the system frequency expressed in Hz can be obtained as:

$$f(t) = [\Delta f(t) + 1] \cdot f_n \quad (17)$$

To validate the accuracy of the proposed frequency response parabolic approximation, the output of the simulation model was used because the actual data and measurements from a competent system operator are not easily accessible. Fig. 4 shows the comparison of the simulated system frequency response and the obtained parabolic approximation. The nominal system frequency f_n is 50 Hz.

TABLE I
COMPARISON BETWEEN f_{min} AND f_{nadir}

$P_L = 0.05$ pu		
System inertia constant H	Parabolic approximation f_{min}	Simulation model f_{nadir}
$H = 1$ s	48.817 Hz	48.617 Hz
$H = 2$ s	49.141 Hz	49.125 Hz
$H = 3$ s	49.299 Hz	49.295 Hz
$H = 4$ s	49.387 Hz	49.382 Hz
$H = 5$ s	49.441 Hz	49.436 Hz
$H = 6$ s	49.478 Hz	49.474 Hz
$H = 7$ s	49.505 Hz	49.502 Hz
$H = 8$ s	49.525 Hz	49.524 Hz
$H = 9$ s	49.541 Hz	49.542 Hz
$H = 10$ s	49.554 Hz	49.558 Hz

Note that a parabola is translated two units horizontally to the right since the load disturbance is set to occur in the 2nd second. It can be seen that the parabola follows the frequency response curve almost perfectly. Furthermore, in the system response analysis, the main goal for developing a parabolic approximation was to preserve the value of the frequency nadir. To clarify, the minimum of the quadratic equation is denoted as f_{min} and the minimum of the system frequency response is denoted as f_{nadir} .

Additionally, the comparison of the system response for different values of H between f_{nadir} , obtained by simulations in MATLAB/Simulink, and f_{min} , obtained by calculating the minimum value of the approximation function, was done and shown in Table I. For the typical values of system inertia ($H = 3$ to $H = 8$ s), the f_{min} deviations from f_{nadir} are less than 0.01 Hz which is insignificant in the practical applications.

One of the most important advantages of this method is that adding power plants to the system does not make the calculation more complex. Namely, by observing (11), one can conclude that each new power plant comes into calculation simply as an additional factor of the sum $SYS(s)$ (equation (12)). Because of the linear property of the inverse Laplace transform, the calculation does not get more complicated.

III. DETERMINATION OF REQUIRED MINIMUM PV POWER RESERVE

To determine the required minimum PV power reserve for participation in the system frequency control, while maintaining the satisfactory inertial response, an appropriate margin of PV power reserve needs to be defined. The problem is examined from the system operator's standpoint. The determination of the de-loaded margin of the PV system is carefully aimed to maximize the contribution to the system frequency control with the minimally possible de-loaded margin. Therefore, our definition of the "required" amount of reserves is primarily related to the frequency response and the stability of the system by finding the point at which the tradeoff between the ability to provide the reserve and efficient energy production is the most optimum. The specific costs and profitability in general are not analyzed here.

The displacement of the conventional power plants by PVs inevitably leads to a reduction of synchronous inertia which causes faster frequency dynamics and, consequently, the appearance of lower f_{nadir} values. However, if the PV systems participate in the system frequency control, the frequency stability is maintained since the PV system provides a very fast dynamic response. The larger the PV power reserve is maintained the better frequency response can be achieved. Therefore, the paramount question is what amount of the power reserve should the PV systems maintain? The genesis for determining the amount of reserves, which is in this paper referred to as "required minimum PV reserve", is based on the following:

- i) If the power system consisting only of the conventional power plants is analyzed and the event of load disturbance P_L occurs, the frequency drop will be stopped at a certain value marked as $f_{nadir-conv}$
- ii) By displacing a share of the conventional generators with the PV power plants the frequency stability is deteriorated mainly due to the decrease of system inertia. This leads to a lower value of the maximum frequency drop $f_{nadir-RES}$ in the case of the same load disturbance P_L :

$$f_{nadir-RES} < f_{nadir-conv} \quad (18)$$

- iii) By including PV production units in the frequency control the values of the frequency nadir can be preserved. The goal of the analysis was to determine the precise amount of the reserve the PV power plant should maintain to achieve the identical system response as the system with a lower share of PV production while considering the same load disturbance P_L :

$$f_{nadir-RES} = f_{nadir-conv} \quad (19)$$

The analyzed power system is the very same power system already described consisting of one thermal power plant and three hydropower plants. The case in which the third hydropower plant is replaced with the PV power plant ($P_{PV} = 200$ MW) is investigated. In this paper, although the transfer function of the PV power plant described by equation (8) is derived for the specific PV power plant with the nominal power 2 kW. The same transfer function can be used for the PV power plant with a greater nominal power since the sum of many small PV power plants can be observed as one aggregated large-scale PV power plant.

First, to analyze and determine the required minimum PV power reserve, the coefficients of a parabola a , b , and c for the base system without the PV power plant were obtained. Recalling (13) and using already obtained values (Section II-C) for this power system $t_1 = 0.1$, $t_2 = 2.2$, and $t_3 = 3.2$, the system of three equations was obtained. By solving the equations, the coefficients a , b , c are obtained as a function of the load disturbance and the system inertia (P_L, H):

$$a_{base} = P_L \frac{7.62H - 0.88}{16.27H^3 + 7.38H^2 + 10.43H - 0.25} \quad (20)$$

$$b_{base} = -P_L \frac{8.14H^2 + 14.90H - 2.07}{16.27H^3 + 7.38H^2 + 10.43H - 0.25} \quad (21)$$

$$c_{base} = P_L \frac{1.04H - 0.74}{16.27H^3 + 7.38H^2 + 10.43H - 0.25} \quad (22)$$

Second, since a_{base} , b_{base} , and c_{base} are the quadratic equation coefficients, a function minimum, i.e., a frequency minimum, can be easily determined as:

$$\Delta f_{min-base}(H, P_L) = c_{base} - \frac{b_{base}^2}{4a_{base}} \quad (23)$$

$$f_{min-base}(H, P_L) = [\Delta f_{min-base}(H, P_L) + 1] \cdot f_n \quad (24)$$

Third, the coefficients of a parabola a , b , and c should be found for the power system with the addition of the PV power plant. To consider the limitation of the maximum PV power, i.e., amount of PV power reserve while performing the simulations in MATLAB/Simulink, the saturation block was used. However, the saturation block is a highly nonlinear element and there were difficulties in representing it by an analytical expression. To overcome the problem, this paper proposes the use of Heaviside step function $u(t)$ which is defined as:

$$u(t) = \begin{cases} 0, & t < 0 \\ 1, & t = 0 \end{cases} \quad (25)$$

Accordingly, the PV power response can be mathematically described as:

$$P_{PVPP}(t) = \mathcal{L}^{-1}\{-F_{ass}(s) \cdot PV(s)\} \cdot [u(t) - u(t-d)] + \frac{P_r}{100} \frac{P_{PV}}{P_B} u(t-d) \quad (26)$$

$$PV_{new}(s) = \mathcal{L}[P_{PVPP}(t)]/F_{ass}(s) \quad (27)$$

where P_r is the PV power reserve in [%]; P_{PV} is the nominal power of PV [MW]; P_B is the base system power [MW]; d is a moment at which PV power reaches its maximum power output; \mathcal{L} is Laplace transform; PV_{new} is the transfer function of the PV system considering the limitation of the power reserve. Given just the injection of the power reserve, stemming from (26), the following can be concluded:

- 1) from $t = 0$ to $t = d$, a PV power plant increases the power from 0 to P_r ;
- 2) at a moment $t = d$, a PV power plant reaches maximum power output;
- 3) for $t > d$, PV power plant continues to operate at power P_r .

In the conducted simulation case, d was set to the value of 0.150 seconds. In this analysis, the value of d can be set freely and be explained with two facts. The first fact is that a moment at which PV power plant reaches its maximum power output can be adjusted by changing the PV plant droop constant (R_{pv}). The second, and the more important fact, is that the frequency nadir is not affected by the change of R_{pv} . This trend is shown in Fig. 5, which depicts the graph of frequency nadir as a function of droop constant R_{pv} . The analysis was conducted for the system parameters: $P_L = 0.05$ pu, $H = 4$ s, $P_r = 5\%$ (0.01 pu). It is evident that the change of frequency nadir is insignificant for the wide range of values of the PV droop constant R_{pv} (2%-10%).

Considering these facts, a parabola for the analyzed power system was developed. Due to the differences in the number and the types of generating units compared to the base power

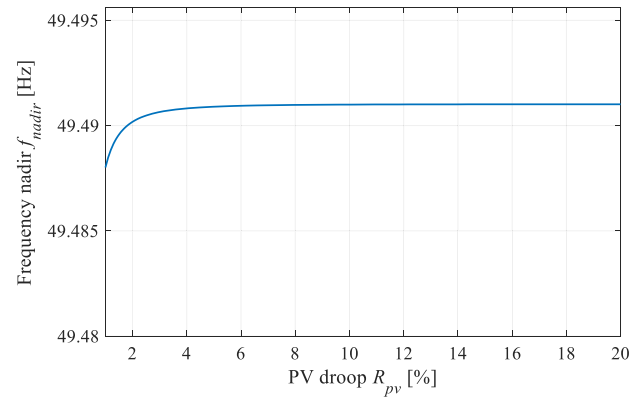


Fig. 5. Frequency nadir as a function of PV droop constant R_{pv} .

system, new values of t_1 , t_2 , and t_3 , for this changed system had to be found. Using the method described in Section II the values of t_1 , t_2 , and t_3 were obtained. However, in this case, the same values as the previous ones, i.e., $t_1 = 0.1$, $t_2 = 2.2$ and $t_3 = 3.2$ were obtained. Again, recalling (13), and solving the system of three equations, the coefficients a , b , c were obtained as a function of P_L , H , and P_r :

$$a = \frac{12021.38P_L - 59.17P_r + 3.12H^2P_r - 354.72HP_r + 190120.56HP_L}{406875H^3 + 262367.03H^2 + 301596.95H + 50732.79} \quad (28)$$

$$b = \frac{-18930P_L + 122.8P_r + 390H^2P_r - 203437.5H^2P_L + 814.3HP_r - 409358.5HP_L}{406875H^3 + 262367.03H^2 + 301596.95H + 50732.79} \quad (29)$$

$$c = \frac{-14638.88P_L - 5.81P_r - 39.03H^2P_r - 74.61HP_r + 27539.20HP_L}{406875H^3 + 262367.03H^2 + 301596.95H + 50732.79} \quad (30)$$

Finally, a frequency minimum as a function of H , P_L , and P_r for this system can be calculated:

$$f_{min}(H, P_r, P_L) = \left(c - \frac{b^2}{4a} + 1\right) \cdot f_n \quad (31)$$

IV. RESULTS

According to the definition for the required minimum PV power reserve given by (19), the equations (24) and (31) are equalized:

$$f_{min}(H, P_r, P_L) = f_{min-base}(H, P_L) \quad (32)$$

Since an increase in the number of PV power plants that substitute synchronous generators leads to a decrease in the system inertia, (32) can be rewritten as:

$$f_{min}(H_n, P_r, P_L) = f_{min-base}(H, P_L) \quad (33)$$

$$H_n = \frac{k}{100} \cdot H \quad (34)$$

where H_n is the decreased system inertia constant, and k is the reduction coefficient [%].

For the three different cases of decreased system inertia, $k = 90\%$, $k = 80\%$, and $k = 70\%$ and $P_L = 0.05$ pu, the determined required minimum of PV power reserve is shown in Fig. 6.

If the inertia constant for the base system is selected to be $H = 5$ s, and if after connecting the PV power plant the inertia constant is decreased by 20% (i.e., $H_n = 80\%$ of H),

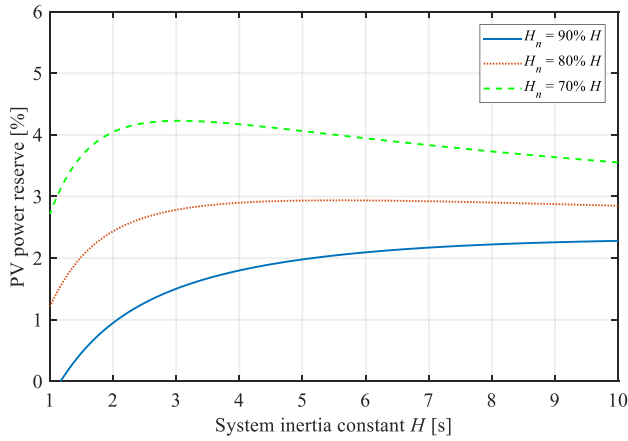


Fig. 6. Required amount of PV power reserve for the different levels of decreased inertia.

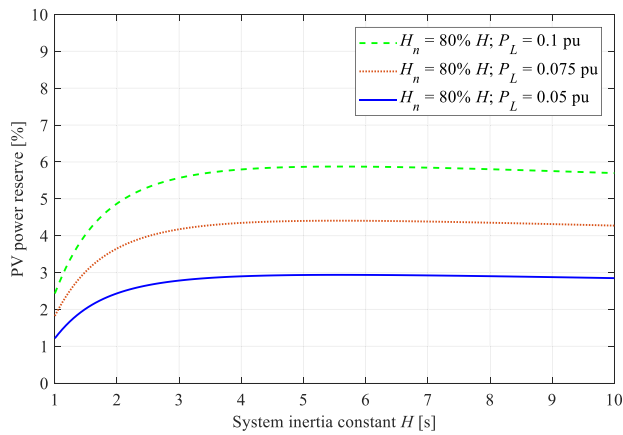


Fig. 7. Required minimum amount of PV power reserve for the different load disturbances.

which corresponds to the previously analyzed case in which the third hydropower plant is replaced by the PV power plant, the maximum amount of PV power reserve does not exceed 3% of nominal power.

It is noteworthy to point out these results were obtained by examining situations where hydropower plant production was replaced by the PV power plants. The results for the required minimum PV power reserve would be higher in the case of observing the thermal power plant displacement because the initial response of these is superior to the hydropower plants. However, the thermal power plants are usually not turned on and off during a day in which they need to provide power since their start-up and shut-down times and the operating costs are high. Thus, this case was not examined in the paper.

The required minimum amount of PV power reserve was also determined in the case of 20% decreased system inertia ($H_n = 80\% H$) for the different load disturbances, $P_L = 0.05 pu$, $P_L = 0.075 pu$, $P_L = 0.1 pu$, and the results are shown in Fig. 7.

It can be seen that the required amount of PV power reserve increases as the magnitude of disturbance increases. However, the maximum amount of required PV power reserve is still

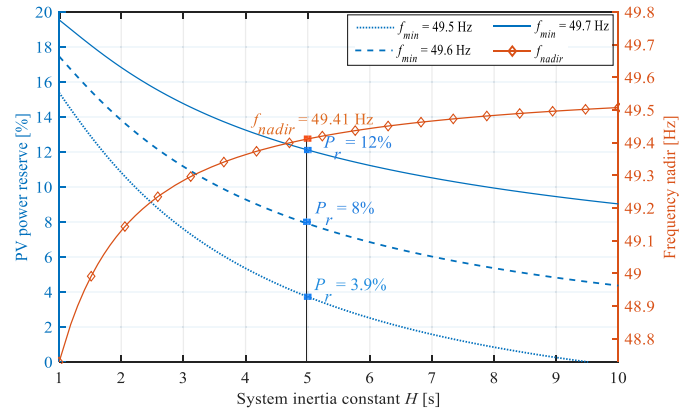


Fig. 8. Required level of PV power reserve P_r to maintain a frequency nadir at the desired value.

below 10% of the nominal power even in the case where the total load was changed by 10% ($P_L = 0.1 pu$).

Additionally, using (31), the required capacity of P_r to maintain a frequency nadir at the desired value for the various values of system inertia was determined. The analysis was conducted for three different values of the minimum allowed frequency ($f_{min} = 49.50 Hz$, $f_{min} = 49.60 Hz$ and $f_{min} = 49.70 Hz$) and results are shown in Fig. 8. A step load disturbance P_L is set to 0.05 or 5% of the total load.

The orange curve in Fig. 8 represents the values of the frequency nadir for the same system but without the PV participation in the system frequency control. If the system with $H = 5s$ is considered in the case without PV participation in the system frequency control, it can be seen that the frequency nadir is $f_{nadir} = 49.41 Hz$. However, if f_{nadir} is raised to 49.50 Hz, 49.60 Hz, or 49.70 Hz, in the case where the PV power plant participates in the system frequency control, then the PV power plant would need to be de-loaded for 3.9%, 8%, and 12% of the nominal power respectively. Fig. 8 also shows that the higher the system inertia is, the lower PV power reserve is required to maintain the frequency nadir at the desired value. This is due to the slower frequency decline at higher H , which provides more reaction time for the remaining generating units.

V. CONCLUSION

In this paper, an approach to determine the required minimum power reserve of the PV systems participating in the system frequency control was presented. The new approach is based on the derivation of the frequency nadir as an explicit function of the system parameters (i.e., system inertia, load disturbance, and PV power reserve). To actualize the proposed approach, parabolic approximation of the system frequency response was developed. The approximation focuses on preserving the values of the frequency nadir as this is considered the key indicator of the frequency response quality. The advantage of the proposed parabolic approximation is that it has only one extreme value corresponding to the real frequency nadir which is easily determined if the coefficients of the quadratic function are known. The analyzed power

TABLE II
HYDROPOWER AND THERMAL POWER PLANTS PARAMETERS

Parameters	HPP1	HPP2	HPP3	TPP1
Nominal power	250 MW	250 MW	200 MW	300 MW
Inertia constant H	5 s	4 s	4 s	6 s
Droop R_{HT}	5%	5%	5%	5%
Governor time constant T_G	0.2 s	0.2 s	0.2 s	0.2 s
Reset time T_R	6 s	6.5 s	7 s	-
Transient droop R_T	0.5 s	0.5 s	0.5 s	-
Turbine time constant T_W	1.05 s	1.10 s	1.00 s	-
Reheater time constant T_{RH}	-	-	-	7 s
Control valve time constant T_{CH}	-	-	-	0.25 s
Fraction of the power in the high-pressure steam turbine F_{HP}	-	-	-	0.35

TABLE III
PHOTOVOLTAIC POWER PLANT PARAMETERS [11]

Parameters	Value [unit]
Nominal power	2 kW
Droop R_{pv}	5%
Input capacitance C	470 μ F
Converter inductance L	500 μ H
DC link voltage V_{DC}	700 V
Time delay constant T_d	50 μ s
PI controller proportional constant K_p	0.01
PI controller integral constant K_i	5.0
Dynamic resistance r_{pv}	-3 Ω
PV current I_{pv}	6.8 A
PV voltage V_{pv}	300 V

system had a total capacity of 1 GW and consisted of one thermal power plant and three hydropower plants. The calculation of the required PV power reserve was based on a novel frequency response parabolic approximation, assuming various levels of inertia reduction due to the grid connection of the PV system (10%, 20%, and 30%). The results showed that in the case of a 20% inertia reduction and a load disturbance of 0.05 pu, the maximum required PV power reserve does not exceed 3% of the nominal power. Although the results may vary for a different system or system topology, this research provides a basis for determining the minimum required PV power reserve regardless of the changes within the system.

Future research could focus on obtaining an analytical expression of the frequency nadir function for a multi-area power system. In this case, the tie-line power flow must be considered, which would increase the accuracy of the

approach. At this stage, we plan to obtain the real system data for our validation study.

APPENDIX

See Tables II and III.

ACKNOWLEDGMENT

This document has been produced with the financial assistance of the European Union. The contents of this document are the sole responsibility of the authors and can under no circumstances be regarded as reflecting the position of the European Union.

REFERENCES

- [1] IEA PVPS TCP. *Photovoltaic Power Systems Programme: Annual Report 2019*. Accessed: Nov. 16, 2020. [Online]. Available: <https://iea-pvps.org/wp-content/uploads/2020/05/IEA-PVPS-AR-2019-1.pdf>
- [2] S. Eftekharijad, V. Vittal, Heydt, B. Keel, and J. Loehr, "Impact of increased penetration of photovoltaic generation on power systems," *IEEE Trans. Power Syst.*, vol. 28, no. 2, pp. 893–901, May 2013.
- [3] X. Huang, K. Wang, and G. Li, "Virtual inertia based control of two-stage photovoltaic inverters for frequency regulation in islanded micro-grid," *Proc. IEEE Power Energy Soc. Gen. Meeting (PESGM)*, Portland, OR, USA, 2018, pp. 1–5.
- [4] S. Adhikari and F. Li, "Coordinated V-f and P-Q control of solar photovoltaic generators with MPPT and battery storage in microgrids," *IEEE Trans. Smart Grid*, vol. 5, no. 3, pp. 1270–1281, May 2014.
- [5] P. Mercier, R. Cherkaoui, and A. Oudalov, "Optimizing a battery energy storage system for frequency control application in an isolated power system," *IEEE Trans. Power Syst.*, vol. 24, no. 3, pp. 1469–1477, Aug. 2009.
- [6] D. Mejía-Giraldo, G. Velásquez-Gomez, N. Muñoz-Galeano, J. Cano-Quintero, and S. Lemos-Cano, "A BESS sizing strategy for primary frequency regulation support of solar photovoltaic plants," *Energies*, vol. 12, no. 2, p. 317, Jan. 2019.
- [7] M. Yue and X. Wang, "Grid inertial response-based probabilistic determination of energy storage system capacity under high solar penetration," *IEEE Trans. Sustain. Energy*, vol. 6, no. 3, pp. 1039–1049, Jul. 2015.
- [8] S. Chen, T. Zhang, H. B. Gooi, R. D. Masiello, and W. Katzenstein, "Penetration rate and effectiveness studies of aggregated BESS for frequency regulation," *IEEE Trans. Smart Grid*, vol. 7, no. 1, pp. 167–177, Jan. 2016.
- [9] A. Sangwongwanich, Y. Yang, F. Blaabjerg, and D. Sera, "Delta power control strategy for multistring grid-connected PV inverters," *IEEE Trans. Ind. Appl.*, vol. 53, no. 4, pp. 3862–3870, Jul./Aug. 2017.
- [10] A. Sangwongwanich, Y. Yang, F. Blaabjerg, and H. Wang, "Benchmarking of constant power generation strategies for single-phase grid-connected photovoltaic systems," *IEEE Trans. Ind. Appl.*, vol. 54, no. 1, pp. 447–457, Jan./Feb. 2018.
- [11] E. I. Batzelis, G. E. Kampitsis, and S. A. Papathanassiou, "Power reserves control for PV systems with real-time MPP estimation via curve fitting," *IEEE Trans. Sustain. Energy*, vol. 8, no. 3, pp. 1269–1280, Jul. 2017.
- [12] X. Li, H. Wen, Y. Zhu, L. Jiang, Y. Hu, and W. Xiao, "A novel sensorless photovoltaic power reserve control with simple real-time MPP estimation," *IEEE Trans. Power Electron.*, vol. 34, no. 8, pp. 7521–7531, Aug. 2019.
- [13] B.-I. Craciun, T. Kerekes, D. Sera, and R. Teodorescu, "Frequency support functions in large PV power plants with active power reserves," *IEEE J. Emerg. Sel. Topics Power Electron.*, vol. 2, no. 4, pp. 849–858, Dec. 2014.
- [14] G. Bao, H. Tan, K. Ding, M. Ma, and N. Wang, "A novel photovoltaic virtual synchronous generator control technology without energy storage systems," *Energies*, vol. 12, no. 12, p. 2240, Jun. 2019.
- [15] X. Lyu, Z. Xu, J. Zhao, and K. P. Wong, "Advanced frequency support strategy of photovoltaic system considering changing working conditions," *IET Gener. Transm. Distrib.*, vol. 12, no. 2, pp. 363–370, Jan. 2018.

- [16] B. Yang, X. Wang, D. Xie, and Y. Guo, "Novel control strategy of grid-connected photovoltaic power supply for frequency regulation," *J. Eng.*, vol. 2019, no. 16, pp. 1488–1491, Mar. 2019.
- [17] C. Loutan *et al.*, "Demonstration of essential reliability services by a 300-MW solar photovoltaic power plant," Nat. Renew. Energy Lab., Golden, CO, USA, Rep. NREL/TP-5D00-67799, 2017.
- [18] S. Liao, J. Xu, Y. Sun, Y. Bao, and B. Tang, "Wide-area measurement system-based online calculation method of PV systems de-loaded margin for frequency regulation in isolated power systems," *IET Renew. Power Gener.*, vol. 12, no. 3, pp. 335–341, Feb. 2018.
- [19] S. I. Nanou, A. G. Papakonstantinou, and S. A. Papathanassiou, "A generic model of two-stage grid-connected PV systems with primary frequency response and inertia emulation," *Electr. Power Syst. Res.*, vol. 127, pp. 186–196, Oct. 2015.
- [20] B.-I. Crăciun, T. Kerekes, D. Séra, R. Teodorescu, and U. D. Annakkage, "Power ramp limitation capabilities of large PV power plants with active power reserves," *IEEE Trans. Sustain. Energy*, vol. 8, no. 2, pp. 573–581, Apr. 2017.
- [21] C. Rahmann, C. Mayol, and J. Haas, "Dynamic control strategy in partially-shaded photovoltaic power plants for improving the frequency of the electricity system," *J. Clean. Prod.*, vol. 202, pp. 109–119, Nov. 2018.
- [22] J. Fang, H. Li, Y. Tang, and F. Blaabjerg, "Distributed power system virtual inertia implemented by grid-connected power converters," *IEEE Trans. Power Electron.*, vol. 33, no. 10, pp. 8488–8499, Oct. 2018.
- [23] H. Ahmadi and H. Ghasemi, "Security-constrained unit commitment with linearized system frequency limit constraints," *IEEE Trans. Power Syst.*, vol. 29, no. 4, pp. 1536–1545, Jul. 2014.
- [24] I. Egido, F. Fernandez-Bernal, P. Centeno, and L. Rouco, "Maximum frequency deviation calculation in small isolated power systems," *IEEE Trans. Power Syst.*, vol. 24, no. 4, pp. 1731–1738, Nov. 2009.
- [25] F. Teng, V. Trovato, and G. Strbac, "Stochastic scheduling with inertia-dependent fast frequency response requirements," *IEEE Trans. Power Syst.*, vol. 31, no. 2, pp. 1557–1566, Mar. 2016.
- [26] M. Paturet, U. Markovic, S. Delikaraoglou, E. Vrettos, P. Aristidou, and G. Hug, "Stochastic unit commitment in low-inertia grids," *IEEE Trans. Power Syst.*, vol. 35, no. 5, pp. 3448–3458, Sep. 2020.
- [27] M. Krpan and I. Kuzle, "Dynamic characteristics of virtual inertial response provision by DFIG-based wind turbines," *Electr. Power Syst. Res.*, vol. 178, Jan. 2020, Art. no. 106005.
- [28] P. Kundur, N. J. Balu, and M. G. Lauby, *Power System Stability and Control*. New York, NY, USA: McGraw-Hill, 1994.
- [29] R. Rajan and F. M. Fernandez, "Power control strategy of photovoltaic plants for frequency regulation in a hybrid power system," *Int. J. Electr. Power Energy Syst.*, vol. 110, pp. 171–183, Sep. 2019.
- [30] K. Tuttleberg, J. Kilter, D. Wilson, and K. Uhlen, "Estimation of power system inertia from ambient wide area measurements," *IEEE Trans. Power Syst.*, vol. 33, no. 6, pp. 7249–7257, Nov. 2018.



Tomislav Baškarad (Graduate Student Member, IEEE) received the B.Sc. and M.Sc. degrees in electrical engineering from the Faculty of Electrical Engineering and Computing, University of Zagreb, where he is currently pursuing the Ph.D. degree. His research interests include renewable energy sources with emphasis on photovoltaic plants, mathematical modeling of power systems, frequency stability, and active power control.



Igor Kuzle (Senior Member, IEEE) is a tenured Professor with the Faculty of Electrical Engineering and Computing, University of Zagreb. His scientific interests include electric power systems dynamics and control, maintenance of electrical appliances, smart grids, and integration of renewable energy sources. He received the highest Croatian National Science Award in 2018, for his outstanding contribution in the field of smart grid applications in transmission systems. In 2019, the Croatian Academy of Sciences and Arts recognized him for excellence in the technical field. He is a member of eight editorial journal boards and has been a chairman of several international conferences.



Ninoslav Holjevac (Member, IEEE) received the Ph.D. degree in electrical engineering from the Faculty of Electrical Engineering and Computing, University of Zagreb, in 2019, where he is a Postdoctoral Researcher. He was a Visiting Researcher with Tsinghua University, China, in 2016. His scientific interests include energy system planning and modeling, and power systems dynamics and control.